Available online at www.sciencedirect.com
ScienceDirect
Journal of Molecular Spectroscopy 243 (2007) 194–201
Journal of MOLECULAR SPECTROSCOPY
www.elsevier.com/locate/jms

Emission spectroscopy of atmospheric pressure plasmas for bio-medical and environmental applications

Z. Machala [a,*], M. Janda [a], K. Hensel [a], I. Jedlovský [b], L. Leštinská [a], V. Foltin [c], V. Martišovitš [a], M. Morvová [a]

[a] Department of Astronomy, Earth Physics and Meteorology, Faculty of Mathematics, Physics and Informatics, Comenius University, Mlynská dolina, 84248 Bratislava, Slovakia
[b] Department of Nuclear Physics and Biophysics, Faculty of Mathematics, Physics and Informatics, Comenius University, Mlynská dolina, 84248 Bratislava, Slovakia
[c] Department of Experimental Physics, Faculty of Mathematics, Physics and Informatics, Comenius University, Mlynská dolina, 84248 Bratislava, Slovakia

Received 29 December 2006; in revised form 19 February 2007
Available online 6 March 2007

Abstract

The paper demonstrates several ways of use of the UV–vis optical emission spectroscopy of medium resolution for the diagnostics of atmospheric pressure air and nitrogen plasmas relevant to bio-medical and environmental applications. Plasmas generated by DC discharges (streamer corona, transient spark, and glow discharge), AC microdischarges in porous ceramics, and microwave plasma were investigated. Molecular (OH, NO, CN) and atomic (H, O, N) radicals, and other active species, e.g. N_2 (C, B, A), N_2^+ (B), were identified. The composition of the emission spectra gives insight in the ongoing plasma chemistry. Rotational, i.e. gas, and vibrational temperatures were evaluated by fitting experimental with simulated spectra. Streamer corona, transient spark and microdischarges generate cold, strongly non-equilibrium plasmas (300–550 K), glow discharge plasma is hotter, yet non-equilibrium (1900 K), and microwave plasma is very hot and thermal (~3000–4000 K). Electronic excitation temperature and OH radical concentration were estimated in the glow discharge assuming the chemical equilibrium and Boltzmann distribution (9800 K, 3×10^{16} cm^{-3}). Optical emission also provided the measurement of the active plasma size of the glow discharge, and enabled calculating its electron number density (10^{12} cm^{-3}).

Keywords: Optical emission spectroscopy; Non-thermal plasma; Electrical discharge; Radicals; Excited species; Environmental and bio-medical applications

1. Introduction

Atmospheric pressure plasmas in air and nitrogen generated by electrical discharges present considerable interest for a wide range of environmental, bio-medical and industrial applications, such as air pollution control, waste water cleaning, bio-decontamination and sterilization, material and surface treatment, electromagnetic wave shielding, carbon beneficiation and nanotube growth, and element analysis. Besides measurements of electrical discharge parameters and photo-documentation, optical emission spectroscopy (OES) in UV–vis regions is widely used for plasma diagnostics as non-invasive and *in situ* method. It provides valuable information on excited atomic and molecular states, enables to determine the rotational, vibrational, and electronic excitation temperatures of the plasma and thus the level of non-equilibrium and the gas temperature, and sometimes even the electron temperature [1,2]. In addition, it enables to identify many radicals and active atomic or molecular species and so gives insight in the plasma chemical processes. This enables understanding and optimizing the air or water pollution control processes. Identification of radicals is also of great importance in biological and medical applications in order to understand the mechanisms of bio-inactivation and of the plasma

* Corresponding author.
E-mail address: machala@fmph.uniba.sk (Z. Machala).

0022-2852/$ - see front matter © 2007 Elsevier Inc. All rights reserved.
doi:10.1016/j.jms.2007.03.001

interaction with living cells [3,4]. Excited states are produced mostly by collisions with energetic electrons, and therefore it is assumed that optical emission can provide a measurement of the plasma active size. This is important in plasma shielding and other applications and also enables calculating basic discharge characteristics and so provides understanding of the physical mechanisms.

Detailed OES characteristics of discharge dynamics usually requires spectrometers equipped with costly ICCD cameras with nanosecond time and very high spectral resolution. Such systems enable for example investigations of temporal/spatial streamer or microdischarge dynamics, Stark broadening analysis for obtaining electron densities, or detailed understanding of chemical mechanisms and measurements of excitation and quenching rate constants [1,2,5–7]. Nevertheless, as we present here, a lot of valuable information on the continuous DC and even on AC or pulsed discharges can be obtained with a relatively cheap spectrometer with medium resolution and long time gates.

We first present OES characterization of three types of DC electrical discharges generating non-thermal plasmas in atmospheric air or nitrogen: streamer corona, transient spark, and glow discharge. They generate non-equilibrium plasmas inducing various chemical end biological effects that are in the interest of polluted air and water cleaning and bio-decontamination. We successfully demonstrated their use for flue air cleaning from organic compounds (VOCs) and for bio-decontamination of some bacteria (*Salmonella typhimurium*, *Bacillus subtilis*, *Bacillus cereus*) [8–11].

We also studied the emission spectra of AC microdischarges in porous ceramic media in atmospheric pressure air, and nitrogen/oxygen mixtures. The microdischarges produce a large density of energetic electrons and free radicals at relatively low energy consumption; so they represent a potential method for car exhaust cleaning [12,13]. Their chemical effects can be even enhanced when the discharge plasma is combined with catalysts, typically of pellet bed type or of honeycomb structure.

Finally we investigated the emission spectra of atmospheric pressure microwave plasma in nitrogen without/with admixtures [14], which can be used for various environmental or industrial applications, such as flue gas cleaning, carbon benefication, surface treatment, and element analysis. Similar MW plasma was used for carbon nanotube growth, and OES was employed as the key diagnostics as well [15]. We tested this plasma for the benefication of waste carbon resulting from used tyre pyrolysis [16].

2. Experiment

2.1. Emission spectroscopy

The experimental set-ups for DC and AC discharges, and MW plasma are shown in Figs. 1 and 2, respectively. The light emitted from the discharges was lead through the optical system consisting of a He–Ne laser for the alignment, an iris and one or two lenses, and focused on the entrance of either the Y-type optic fiber, or through a beamsplitter to two optic fibers positioned at 90°. A two-channel spectrometer Ocean Optics SD2000 (Master 200–500 nm, spectral resolution 0.6 nm; and Slave 500–1100 nm, resolution 1.2 nm) was used for the optical emission diagnostics. The minimum time gate of the CCD array on the spectrometer was 3 ms but in most cases we integrated spectra over 1 s or more. The best spatial resolution was 0.2 mm. The optical system was calibrated by tungsten and deuterium lamps traceable to NIST calibration standards.

2.2. Discharge characteristics

Three types of DC electrical discharges generating non-thermal plasmas in atmospheric air or nitrogen were investigated: a well known streamer corona (SC), and a relatively novel transient spark (TS) and glow discharge (GD); both in more detail described in [8–11]. We tested these discharges in both polarities between two metal electrodes, or with one electrode immersed in water, which simulates conditions of the discharge action on biological media in water solution. SC and TS are pulsed discharges despite the DC applied voltage.

SC is typical with small current pulses (~10 mA) with a repetitive frequency of 10–30 kHz, during which the discharge voltage remains fairly constant. TS is a repetitive streamer-to-spark transition discharge. The voltage drops to zero during the high current pulses (~1 A) with typical repetitive frequency of 0.5–5 kHz. Thanks to the very short spark pulse duration (~100 ns) given by a small internal capacity of the discharge chamber and a limiting series resistor, the plasma cannot reach LTE conditions [8]. On the other hand, the periodic streamer-to-spark transition provides non-equilibrium conditions with fast electrons resulting in efficient chemical and biological cleaning effects. GD has constant voltage and current (~1–10 mA), and a descending current–voltage characteristics, described in detail in [9,10]. It is pulseless thanks to the appropriate series resistor that prevents its transition to spark but allows small current. With the current increasing above some ~100–1000 mA, the discharge smoothly transits towards an arc.

Here we show the emission spectra of the DC discharges in a 4 mm gap (distance between the high voltage needle electrode and the water level); SC: repetitive frequency 26 kHz, current pulse amplitude $I_{max} = 25$ mA; TS: 1 kHz, $I_{max} = 1.5$ A; GD: $I = 6$ mA.

AC and DC microdischarges (MD) in porous ceramic media in atmospheric pressure air and nitrogen/oxygen mixtures were in more detail described in [12,13]. The pore size and the thickness of the tested ceramics were 2–200 μm and 3–7 mm, respectively. The MD electric and optical characteristics depend very much on the pore size, discharge power, gas mixture composition and gas flow rate. At a small voltage (e.g. up to 10 kV for 7 mm thick ceramics) or for very small pores (<2 μm), a surface discharge over the ceramics surface was observed. With an increasing

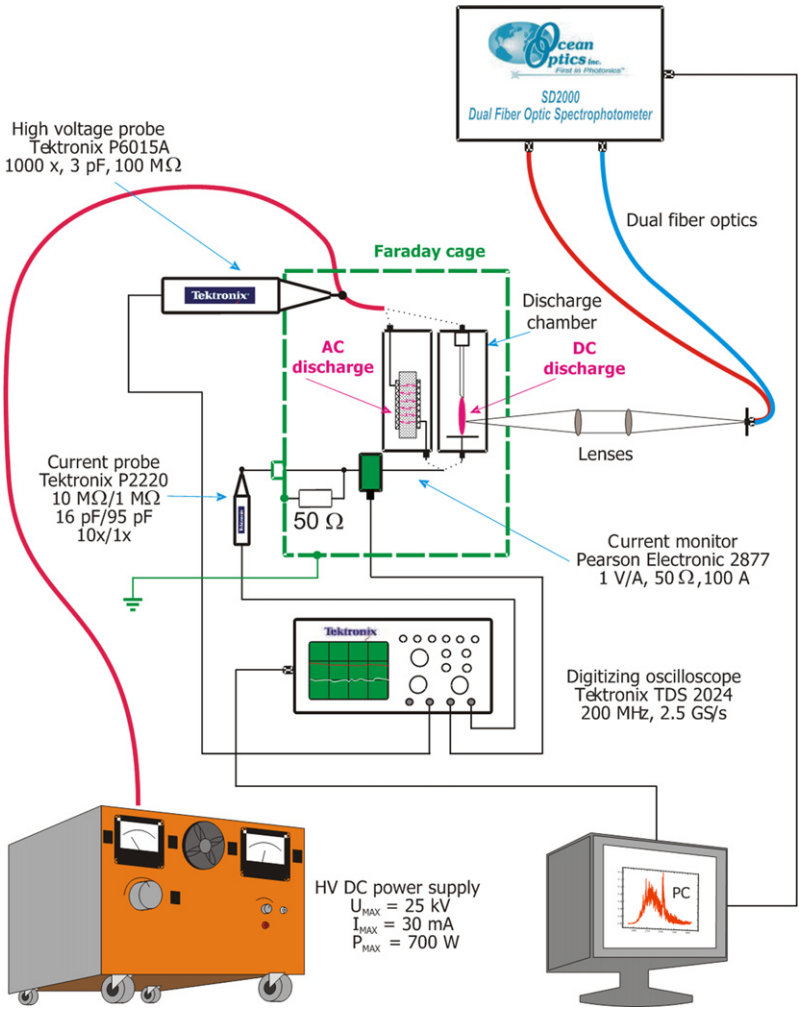

Fig. 1. Experimental set-up for DC and AC discharge experiments and emission spectroscopy.

applied voltage, microdischarges inside the ceramics were formed. The onset voltage of MD increased with the decreasing pore size. For a given voltage, the MD total current increased with the pore size. The amplitude (~10–35 A) and the frequency (~kHz) of the current pulses increased with the MD mean current. The maximal amplitude of the pulses was observed for 50 and 80 μm pore sizes, while the frequency was relatively independent of the pore size.

Atmospheric pressure microwave (MW) plasma generated by Litmas Red plasma torch (2.45 GHz, 3 kW) in nitrogen without/with admixtures was finally investigated. The torch can generate plasmas in the temperature range 750–4700 K, the gas flow rates 8–110 l/min and magnetron powers up to 3 kW.

3. Results and discussion

3.1. Identification of species in the emission spectra

The typical emission spectra of the three types of DC discharge are shown in Figs. 3 and 4. As usual with atmospheric air non-equilibrium discharges, N_2 spectra were dominant. In equilibrium (LTE) plasmas they appear only when gas temperature reaches 6000 K [1]. Spectrum of N_2 2nd positive system ($C^3\Pi_u$–$B^3\Pi_g$) in UV was typically accompanied by the N_2 1st positive system ($B^3\Pi_g$–$A^3\Sigma_u^+$) in vis indicating the formation of N_2 $A^3\Sigma_u^+$ states. These long-lived metastables (energy ~6 eV) are important as reservoirs of energy promoting plasma chemical reactions leading to condensed products in flue gas cleaning applications [8], although their lifetime in air plasmas is rather short due to collisional quenching by oxygen. On the other hand, N_2 $A^3\Sigma_u^+$ plays an important role in discharges in N_2–CO_2 and N_2–CO_2–H_2O mixtures, enabling formation of amino acids and other organic species that were probably involved in the chemical evolution of life on the Earth [17].

Emission of OH ($A^2\Sigma^+$–$X^2\Pi_{3/2}$) and NO γ ($A^2\Sigma^+$–$X^2\Pi_r$) systems in UV are also often observed in air plasmas. OH radical is formed from water vapors present in the ambient air. In our discharges with water electrode, water was evaporated directly. NO radical was formed from O_2 and N_2 that dissociate at higher temperatures (>1600 K) or by electron impact. NO and OH radicals were detected mainly in GD. They play crucial roles in biochemi-

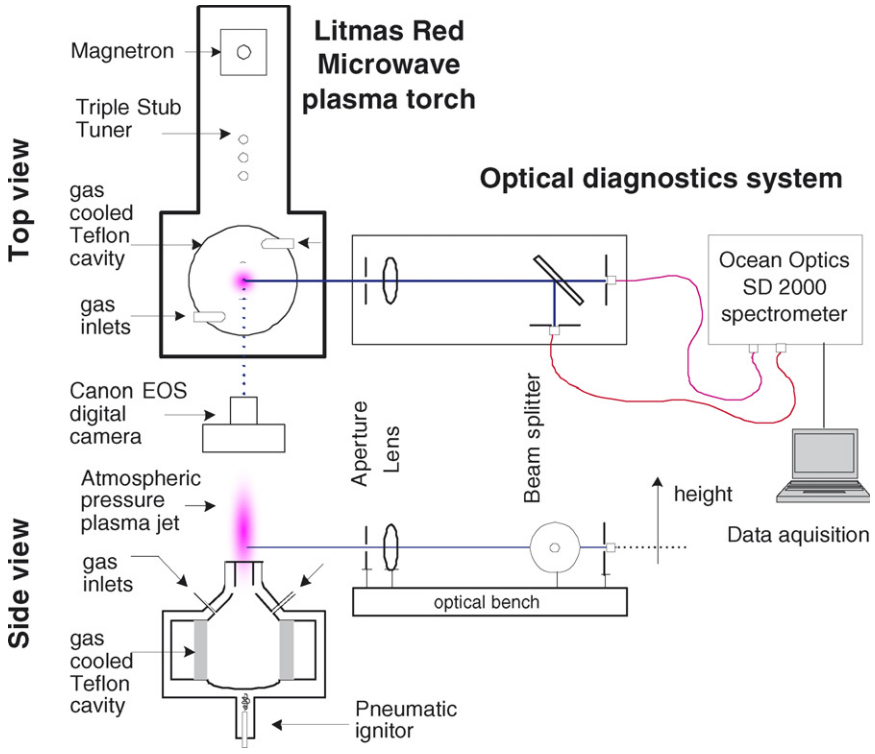

Fig. 2. Experimental set-up for MW plasma experiments and emission spectroscopy.

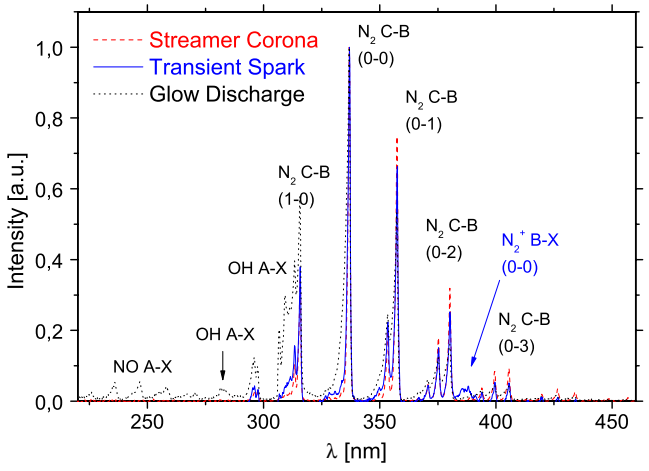

Fig. 3. Typical emission spectra of DC discharges in UV region (corrected for the spectrometer's spectral response). Gap: 4 mm; SC: 26 kHz, $I_{max} = 25$ mA; TS: 1 kHz, $I_{max} = 1.5$ A; GD: $I = 6$ mA.

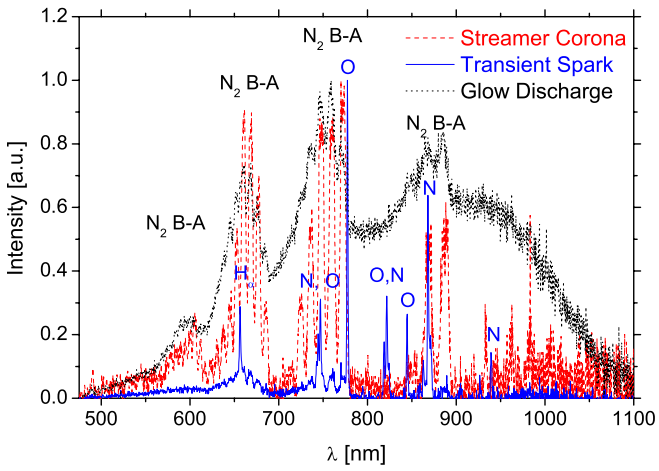

Fig. 4. Typical emission spectra of DC discharges in vis–NIR region (corrected for the spectrometer's spectral response). Gap: 4 mm; SC: 26 kHz, $I_{max} = 25$ mA ; TS: 1 kHz, $I_{max} = 1.5$ A; GD: $I = 6$ mA.

cal decontamination, sterilization and water cleaning applications due to their strong reactivity and bactericidal effect.

Plasmas with high electron temperatures (i.e. energies) give the emission of N_2^+ 1st negative system ($B^2\Sigma_u^+$–$X^2\Sigma_g^+$) and atomic N, O, and H lines, as could be observed in TS, as well as in MD. These species indicate a high level of non-equilibrium and the presence of energetic electrons that initiate dissociations and ionizations, essential in air and water cleaning, as well as in bio-decontamination. Atomic N, O, and H radicals initiate further plasma chemical processes, such as formation of ozone (O_3), peroxyl radicals (HO_2), and many other reactive species. MD demonstrated additional atomic lines and molecular bands in the emission spectra resulting from the ceramic material.

Emission spectra of MW plasmas generated by the plasma torch in nitrogen were composed of CN violet ($B^2\Sigma^+$–$X^2\Sigma^+$) and red ($A^2\Pi$–$X^2\Sigma^+$) systems. CN radicals are formed in N_2 from carbon-containing impurities. There were no N_2 spectra detected because the electron energy in this plasma was too weak to electronically excite N_2 molecules. A very small admixture of oxygen or water vapor

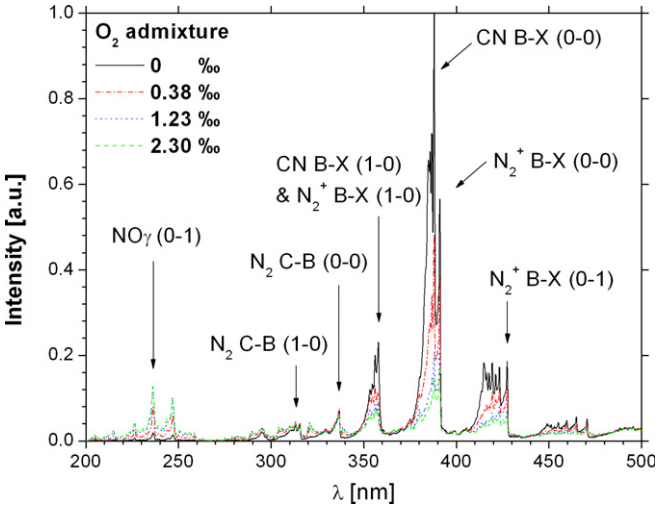

Fig. 5. UV emission spectra of MW plasma in nitrogen with small O_2 admixture. $P = 1.46$ kW, $Q = 26$ l/min.

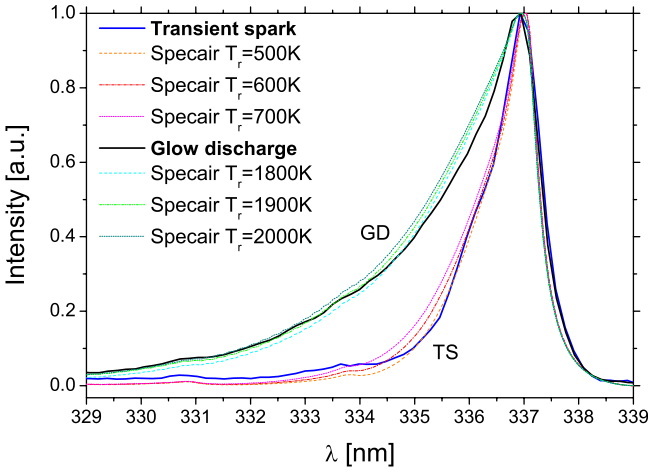

Fig. 6. Determination of rotational temperatures from N_2 2nd positive system (corrected for the spectrometer's spectral response). Gap: 4 mm; TS: 1 kHz, $I_{max} = 1.5$ A; GD: $I = 6$ mA.

(~100–1000 ppm) in the nitrogen plasma dramatically changed the involved plasma chemistry and thus the emitted spectra, strongly decreasing the CN emission and enhancing the emission of NO or NH radicals, as illustrated in Fig. 5. Similar effect was observed in low pressure afterglow by [4].

3.2. Temperature evaluation from the emission spectra

Spectra of the N_2 2nd positive system ($C^3\Pi_u$–$B^3\Pi_g$) emitted both in air and nitrogen are the most convenient for plasma diagnostics, since they enable to determine rotational T_r and vibrational T_v temperatures by fitting the experimental spectra with the simulated ones. We used SPECAIR [1,18] and LIFBASE [19] software for spectral simulation. Other radiative excited species can be used for this purpose as well, most typically OH [1,20], but also NO or CN. However, they typically overestimate the temperatures due to the fact that these radicals are result of chemical reactions and residual chemical energy can manifest itself by elevating temperatures [2,21]. Fitting the experimental spectra with the simulated ones is shown in Fig. 6.

Owing to fast collisional relaxation at atmospheric pressure, the gas temperature T_g equals with T_r. Vibrational temperature $T_v > T_r$ indicates the non-equilibrium in the plasma, although it may not be well defined in strongly non-equilibrium conditions when vibrational states do not follow the Boltzmann distribution. The temperatures measured in DC discharges with the low-voltage electrode submerged in water were the following:

SC (26 kHz): $T_g \approx T_r = 350 \pm 100$ K, $T_v = 2000 \pm 500$ K
TS (1 kHz): $T_g \approx T_r = 550 \pm 100$ K, $T_v = 3000 \pm 500$ K
GD (6 mA): $T_g \approx T_r = 1900 \pm 100$ K, $T_v = 3500 \pm 200$ K

When no water was present in the discharge chamber, the same discharges at approximately the same parameters gave slightly higher temperatures (about 50 K more in SC and TS, and 100 K in GD). In the humid case, some portion of energy was spent for water evaporation and dissociation.

The evaluated GD temperatures are in a good agreement with other authors who investigated a similar discharge between two metal electrodes [21,22] or even with water electrode [23,24]. T_g of GD is high, because it is a continuous discharge. A large fraction of the electron energy is lost via excitation of the vibrational modes of air molecules, mainly N_2. These vibrational modes subsequently relax through collisions with the dominant species. The collisional quenching transfers the energy from vibration into the translational modes of molecules, which results in Joule heating of the gas. The typical time scales of this vibrational–translational (V–T) energy transfer in atmospheric air are 10–100 μs. In the short pulses of TS, SC or MD (duration ~100 ns), this V–T transfer does not have sufficient time to develop during the discharge pulse. It can only affect the relaxation phase between the pulses. But there, its effect on the gas heating is weak because its time scales are on the contrary much shorter that the typical length of the relaxation period (with the repetitive frequency of some ~1 kHz). Therefore T_g remained fairly low in TS, SC, and MD, despite the electrons had high energies.

Gas temperatures in AC microdischarges in porous ceramics in nitrogen/oxygen mixtures with the typical power of about 3–4 W (16–18 kV) measured by the same way gave the following results:

Pure N_2: $T_g \approx T_r = 300 \pm 50$ K, $T_v = 2000 \pm 300$ K
5% O_2 in N_2: $T_g \approx T_r = 350 \pm 50$ K, $T_v = 2500 \pm 300$ K
20% O_2 in N_2: $T_g \approx T_r = 400 \pm 50$ K, $T_v = 2800 \pm 300$ K

The temperatures increased with the increasing amount of O_2. This is because O_2 is an electronegative gas and so decreases the number of electrons by attachment under formation of negative O^- and O_2^- ions. Higher energy was thus required to sustain the discharge at the same parameters than in nitrogen, resulting in higher temperatures. The

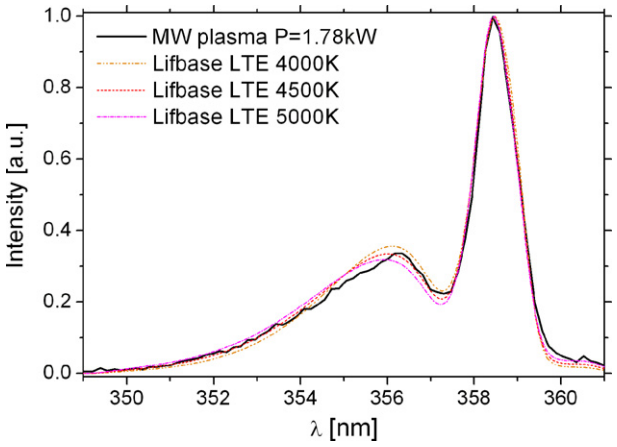

Fig. 7. Determination of rotational temperatures from CN violet spectral bands; $Q = 15$ l/min.

same effect has been observed in our previous experiments with the atmospheric glow discharge [8].

In the MW plasma, the temperatures were evaluated from the CN violet ($B^2\Sigma^+$–$X^2\Sigma^+$) system (Fig. 7), since CN was the only emissive species in this case. This plasma reached 3000–4500 K depending on the microwave power and the gas flow rate, and was close to the local thermal equilibrium (LTE) conditions. We admit that the temperature measured from CN spectra may be overestimated, since CN are radicals formed by chemical reactions. Nevertheless, a high temperature of this plasma is required for applications such as carbon benefication, and was confirmed by desirable structural and composition changes of the treated waste carbon [16].

3.3. Electronic temperature and radical concentration measurement

Spectra with several emission systems enable estimating T_{el}, the electronic excitation temperature, which corresponds to the Boltzmann distribution among excited electronic states. This T_{el} may be close to T_e, the temperature of free electrons. Non-equilibrium plasmas typically have $T_e > T_{el} > T_v > T_r$ [1,21]. We estimated T_{el} in GD that demonstrated N_2 2nd positive, NO γ, and OH systems in the UV spectra. By changing T_{el} in the modeled spectrum, relative intensities of N_2 2nd positive and NO γ systems varied and we found the best fit of the experimental spectrum at $T_{el} = 9800$ K (after having T_r and T_v already determined), as shown in Fig. 8. We may presume T_e higher than T_{el}. In TS, this T_e is most likely even higher due to stronger formation of atomic radicals and N_2^+ ions, as discussed above. Regrettably, T_{el} could not be estimated by this method in TS, since NO γ system was not present and N_2^+ 1st negative was too weak to draw any conclusions. We expect higher T_e also in MD.

Nonetheless, the reliability of this described method is limited, because it is based on N_2 2nd positive and NO γ systems that may not be in chemical equilibrium. NO are radicals formed by chemical pathways, and thus may posses certain chemical energy. They also may not follow the Boltzmann distribution of electronic excited states.

After having $T_g = T_r$, T_v, and presumed T_{el} of GD, and assuming the Boltzmann distribution of all excited electronic states, we can estimate the concentration of OH radicals from the intensity of the OH A–X band. Since OH A–X band partly overlaps with the N_2 2nd positive 1–0 and 2–1 bands, this method is very sensitive to T_{el} and T_v. SPECAIR uses the database of an initial LTE species distribution at various temperatures (not specific to the excitation). In all air modeled spectra we used this database for air with 42% relative humidity. However, even after T_{el} being found, the OH modeled spectrum could not reach the value of the measured intensity of OH bands, since the real concentration of water vapors in the discharge was higher ($T_g = 1900$ K caused a strong water evaporation and dissociation). So we increased the initial OH concentration in this database until a good match with the measured OH bands was reached, as shown in Fig. 9. The corresponding

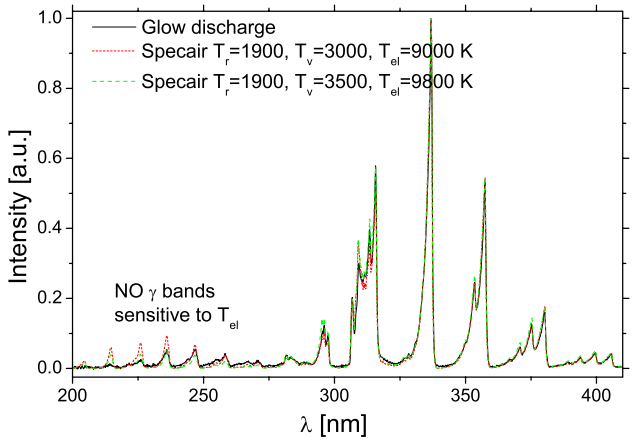

Fig. 8. Estimation of T_{el} from the complex glow discharge spectra (corrected for the spectrometer's spectral response). Gap: 4 mm; $I = 6$ mA.

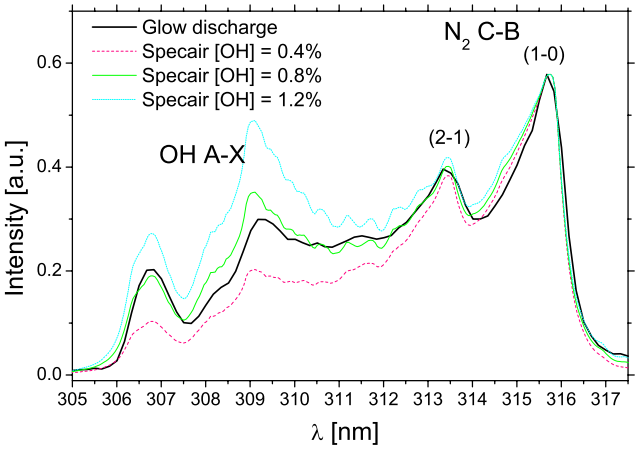

Fig. 9. Fitting OH bands to estimate the OH concentration in the glow discharge (corrected for the spectrometer's spectral response). Gap: 4 mm; $I = 6$ mA.

OH concentration was found: [OH] ≈ 0.8% vol. that (at 1900 K, neutral density $N = 3.86 \times 10^{18}$ cm^{-3}) corresponds to approximately 3×10^{16} cm^{-3}. Keeping in mind the limitations of the determining T_{el} and the Boltzmann distribution assumptions, this calculated OH concentration should be taken as a very rough estimate, just indicating the order of magnitude. However, such concentration is very high and so explains the dominant role of OH radicals in bio-decontamination or flue gas cleaning applications.

3.4. Measurement of the plasma size and electron density

The spatial distributions of the light emitted from the discharge provide useful information on the discharge properties. The 2-dimensional radial-axial emission intensity distributions of GD with the discharge current $I = 5$ mA and gap length 7 mm were recorded at 337 nm (N_2 C–B (0,0) band), as shown in Fig. 10. An intensity peak at the cathode vicinity, as well as the intensity minimum around 2.5–3 mm from the cathode, were distinguished. They can be also observed visually as lighter and darker spaces.

The diameter of the positive column of the discharge can be defined as the full width of half maximum (FWHM) of the radial electron density profile. Although the direct measurement of the electron density in atmospheric pressure plasmas is difficult, the Abel-inverted radial emission intensity profiles of various excited species in the discharge column (most typically N_2 $C^3\Pi_u$–$B^3\Pi_g$) can be used to measure the discharge diameter D. Abel inversion was applied because the discharge has a radial symmetry. Such an approach assumes that the emission profiles agree well with the electron density profile. The discharge diameter measured as the FWHM of the radial emission profiles

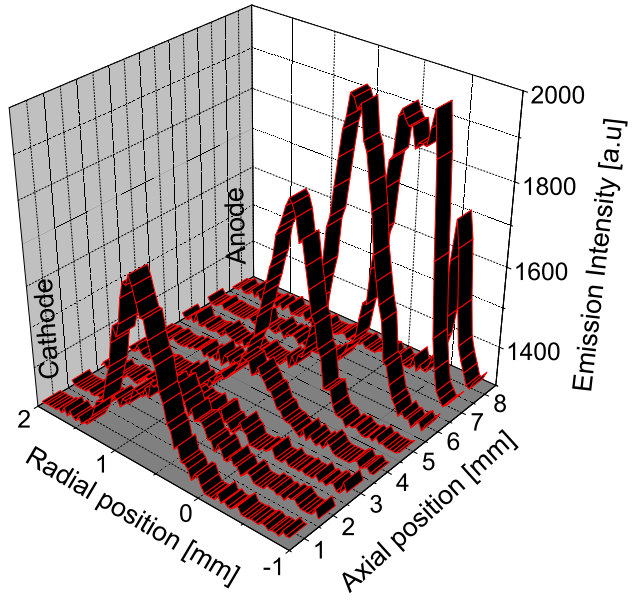

Fig. 10. 2D radial–axial emission intensity profile at $\lambda = 337$ nm (corrected for the spectrometer's spectral response). DC glow discharge in ambient air, $I = 5$ mA, gap 7 mm. Radial profiles at each axial position represent integrated intensity over 1 mm thick axial plasma slab.

than allows estimating the plasma volume. It can also be used to estimate the current density j by using a simplified relation

$$j = \frac{I}{\frac{1}{4}\pi D^2}.$$

The typical GD in ambient air ($I = 5$ mA) has a diameter $D = 0.53$ mm, as measured by emission of the N_2 C–B (0,0) band, with the corresponding $j = 2.3$ A/cm^2.

Electron number density n_e is a very important parameter characterizing the plasma and can be derived from the measured current density and electric field strength. The simplest estimate of n_e can be then obtained using the expression for the current density

$$j = n_e e v_d,$$

where e is the elementary charge and v_d is the electron drift velocity. The electron drift velocity is given by the electron mobility μ_e and the electric field strength E:

$$v_d = \mu_e E.$$

E was approximately measured from the applied voltage and the column length. μ_e, or rather the product of the μ_e and the pressure p, can be considered constant in our experimental conditions (positive column of an air glow discharge): $\mu_e p = 4.6 \times 10^5$ cm^2 Torr V^{-1} s^{-1} [25]. The pressure should be better represented by the gas density N to accommodate for the elevated temperature at $p = 1$ atm, similar to representing the reduced field as E/N rather than E/p. In N-representation, $\mu_e N = 1.484 \times 10^{22}$ cm^{-1} V^{-1} s^{-1} in air glow discharges. This value can be then used in the expression of the electron drift velocity and the electron density can be calculated subsequently:

$$n_e = \frac{j}{e\mu_e N \frac{E}{N}}.$$

Resulting n_e of GD was in the order of 10^{12} cm^{-3}. Measurements of n_e in TS or MD would require a single pulse time-resolved spectroscopy with an ICCD system.

4. Summary

We used optical emission spectroscopy in UV–vis regions for the diagnostics of atmospheric pressure plasmas and discharges relevant to environmental and bio-medical applications. Identification of radicals and other active species in three types of DC discharges and AC microdischarges in ceramics revealed the differences between the types of generated non-equilibrium plasmas, as well as their roles in bio-decontamination and air cleaning processes. Most importantly, OH, NO and atomic H, O, and N radicals were detected. In MW nitrogen plasma, CN radicals were found dominant.

We then applied OES to determine the rotational and vibrational temperatures and thus the level of non-equilibrium and the gas temperatures of the studied plasmas. All studied DC and AC discharges generate non-equilibrium

plasmas. The continuous glow discharge was the hottest one with T_g reaching 1900 K, since most of electron energy is spent for gas heating. The pulsed transient spark, streamer corona and AC microdicharges were relatively cold, with T_g of 300–600 K. Such cold plasmas are the most convenient for energetically efficient air cleaning, as well as for sterilization. The MW nitrogen plasma was close to LTE with high T_g of 3000–4500 K, which is on the other hand required for carbon benefication or other processes.

Spectra of the glow discharge enabled the estimation of the electronic excitation temperature because they contained several molecular systems that were presumed to be in chemical equilibrium and to follow the Boltzmann distribution. T_{el} was estimated to 9800 K, we assume electron temperature higher than that. The concentration of OH radicals was approximated by fitting the OH bands and a very high value of 3×10^{16} cm^{-3} was found.

Optical emission, especially axial and radial emission profiles can also provide a measurement of the plasma active size. We detected non-uniform intensity distribution along the glow discharge axis and measured the typical diameter of the positive column. This allowed calculating the current and electron number densities in the discharge, with typical values of $j = 2.3$ A/cm^2 and $n_e \approx 10^{12}$ cm^{-3}.

In conclusion, we demonstrated several possibilities of the use of OES to characterize atmospheric pressure plasmas relevant bio-medical and environmental applications.

Acknowledgments

This work was carried out under the support from Slovak Grant Agency VEGA 1/2013/05, 1/3041/06, 1/3068/06 and 1/3043/06; NATO EAP.RIG 981194, and Science and Technology Assistance Agency APVT-20-032404 and SK-FR-00506 Grants. We gratefully acknowledge Sencera, Ltd. for loaning us the MW torch. We thank Prof. Christophe O. Laux (Ecole Centrale Paris) for fruitful discussions and for allowing our spectrometer's calibration with his standards.

References

[1] C.O. Laux, T.G. Spence, C.H. Kruger, R.N. Zare, Plasma Sources Sci. Technol. 12 (2003) 125–138.
[2] U. Fantz, Plasma Sources Sci. Technol. 15 (2006) S137–S147.
[3] M. Laroussi, IEEE Trans. Plasma Sci. 30 (2002) 1409–1415.
[4] A.-M. Pointu, A. Ricard, B. Dodet, E. Odic, J. Larbre, M. Ganciu, J. Phys. D: Appl. Phys. 38 (2005) 1905–1909.
[5] K.V. Kozlov, H-E. Wagner, R. Brandenburg, P. Michel, J. Phys. D: Appl. Phys. 34 (2001) 3164–3176.
[6] M. Šimek, V. Babický, M. Člupek, S. DeBenedictis, G. Dilecce, P. Šunka, J. Phys. D: Appl. Phys. 31 (1998) 2591–2602.
[7] M. Šimek, S. DeBenedictis, G. Dilecce, V. Babický, M. Člupek, P. Šunka, J. Phys. D: Appl. Phys. 35 (2002) 1981–1990.
[8] Z. Machala, M. Morvová, E. Marode, I. Morva, J. Phys. D: Appl. Phys. 33 (2000) 3198–3213.
[9] Z. Machala, E. Marode, C.O. Laux, C.H. Kruger, J. Adv. Oxid. Technol. 7 (2004) 133–137.
[10] Z. Machala, E. Marode, M. Morvová, P. Lukáč, Plasma Process. Polym. 2 (2005) 152–161.
[11] Z. Machala, I. Jedlovský, K. Hensel, V. Martisovitš, V. Foltin, Biological Effects of DC Discharges in Atmospheric Air with Water, Int. Symp. High Pres. Low Temp. Plasma Chemistry HAKONE X, 7P-09, 277–283, Saga, Japan, September 2006.
[12] K. Hensel, S. Katsura, A. Mizuno, IEEE Trans. Plasma Sci. 33 (2005) 574–575.
[13] K. Hensel, M. Janda, M. Leštinský, Z. Machala, V. Martišovitš, P. Tardiveau, A. Mizuno, Electrical and Optical Properties of AC Microdischarges in Porous Ceramics, Int. Symp. High Pres. Low Temp. Plasma Chemistry HAKONE X, 1P-05, 41–46, Saga, Japan, September 2006.
[14] V. Foltin, L. Leštinská, Z. Machala, Czech. J. Phys. 56 (2006) B712–B720.
[15] L. Zajíčková, M. Eliáš, O. Jašek, V. Kudrle, Z. Frgala, J. Matějková, J. Buršík, M. Kadlečíková, Plasma Phys. Control. Fusion 47 (2005) 1–12.
[16] L. Leštinská, V. Foltin, M. Zahoran, Z. Machala, Carbon Benefication in Atmospheric Pressure Microwave Plasma, in: 16th Symposium on Applications of Plasma Processes SAPPXVI, Podbanské, Slovakia, January 20-25 (2007) P46, 215–216.
[17] M. Janda, The Study of Plasma Induced Chemistry in Gaseous Mixture N2 -CO2 -H2O, PhD thesis, Comenius University Bratislava 2006.
[18] C.O. Laux, Radiation and Nonequilibrium Collisional-Radiative models von Karman Institute for Fluid Dynamics, Lecture Series 2002–07, in: D. Fletcher, T. Magin, J.-M. Charbonnier, G.S.R. Sarma (Eds.), Rhode Saint-Genese, Belgium, June 4–7, 2002.
[19] J. Luque, D.R. Crosley, SRI Report MP 99-009 (1999).
[20] S.Y. Moon, W. Choe, Spectrochim. Acta B 58 (2003) 249–257.
[21] D. Staack, B. Farouk, A. Gutsol, A. Fridman, Plasma Sources Sci. Technol. 14 (2005) 700–711.
[22] L. Yu, C.O. Laux, D.M. Packan, C.H. Kruger, J. Appl. Phys. 91 (2002) 2678–2686.
[23] X. Lu, F. Leipold, M. Laroussi, J. Phys. D: Appl. Phys. 36 (2003) 2662–2666.
[24] G. Faure, S.M. Shkol'nik, J. Phys. D: Appl. Phys. 31 (1998) 1212–1218.
[25] Yu.P. Raizer, Gas Discharge Physics, Springer, New York, 1991.